Offshore Breakwaters in Laboratory and Field

Article *in* Journal of Waterway Port Coastal and Ocean Engineering · March 1987

DOI: 10.1061/(ASCE)0733-950X(1987)113:2(105)

2 authors:

Kyung-Duck Suh
Seoul National University
163 PUBLICATIONS **1,454** CITATIONS

SEE PROFILE

Robert Anthony Dalrymple
Johns Hopkins University
290 PUBLICATIONS **11,515** CITATIONS

SEE PROFILE

DEL-SG-09-87

OFFSHORE BREAKWATERS IN LABORATORY AND FIELD

by Kyungduck Suh, and Robert A. Dalrymple

This work was sponsored by the
National Sea Grant College Program under
Grant No. NA83AA-D-0017

$1

Reprinted from *Journal of Waterway, Port, Coastal, and Ocean Engineering* Vol. 113, No. 2, March, 1987.

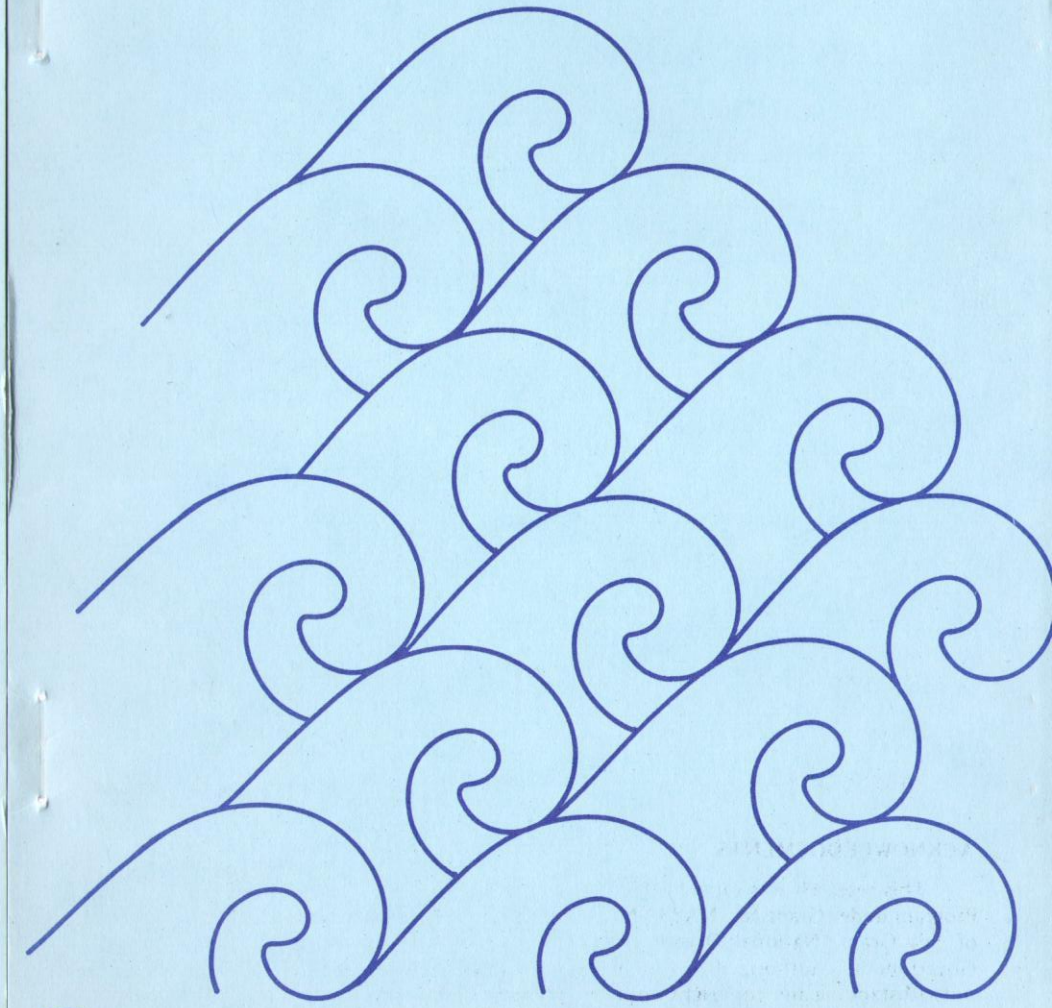

University of Delaware Sea Grant College Program
Newark, Delaware 19716

ACKNOWLEDGEMENTS

This research was supported in part by the University of Delaware Sea Grant College Program under Grant No. NA83AA-D-0017 (Project No. 3-7-21-3120-31), from the Office of Sea Grant, National Oceanic and Atmospheric Administration (NOAA). The U.S. Government is authorized to produce and distribute reprints for governmental purposes, notwithstanding any copyright notation that may appear hereon.

OFFSHORE BREAKWATERS IN LABORATORY AND FIELD

By Kyungduck Suh,[1] S. M. ASCE, and Robert A. Dalrymple,[2] M. ASCE

ABSTRACT: Small-scale model tests for single and multiple offshore breakwaters were performed in a spiral wave basin to examine the effects of their geometric parameters on the morphological change in their vicinity. The model results are compared with physical model studies reported by others and with offshore breakwaters in the field. All the horizontal lengths are nondimensionalized with respect to the offshore distance of the breakwater from the original shoreline, X_B. Three dimensionless variables, X_b^* ($=X_b/X_B$), L_B^* ($=L_B/X_B$), and G_B^* ($=G_B/X_B$), are found to be important, in which X_b, L_B, and G_B are the surf zone width, the length of breakwater, and the gap spacing between adjacent breakwaters, respectively.

INTRODUCTION

Many coastal regions are suffering serious erosion due to sea level rise, the reduction in sediment supply from rivers, and/or the interruption of longshore sediment transport by man-made structures such as jetties. Various kinds of coastal structures, e.g., seawalls, groins, offshore breakwaters, and artificial headlands, have evolved for beach erosion control. Artificial beach nourishment is also used as an alternative method of coastal protection, which provides an additional amenity in the form of a bathing beach. In some places where seawalls and groins are not effective, offshore breakwaters are a means to protect the beach against severe erosion (25,29). Despite the fact that offshore breakwaters are not as popular as groins for beach protection due to their high cost and the difficulty of construction and maintenance, their use has been increased remarkably since 1970 (4,27).

The concept of an offshore breakwater for beach protection is relatively new compared with that of other erosion control measures, so that only a little is known about the hydrodynamics (10,11,14,22) and the resulting sediment transport mechanism in its vicinity. Thus, little information is available for design. It is known that the currents engendered behind the breakwater by the waves deposit sediments in the sheltered area to build a new morphological shape called a salient until a new equilibrium shape of the shoreline is achieved. If the salient touches the breakwater, it is called a tombolo. In the past, many coastal engineers have tried to find the proper design criteria for an offshore breakwater system relating its geometric parameters to the corresponding morphological change by means of physical model tests (1–3, 12,21–24), numerical modeling (13,15,17,20,24), or the investigation

[1]Grad. Student, Dept. of Civ. Engrg., Univ. of Delaware, Newark, DE 19716.
[2]Prof., Dept. of Civ. Engrg., Univ. of Delaware, Newark, DE 19716.

Note.—Discussion open until August 1, 1987. To extend the closing date one month, a written request must be filed with the ASCE Manager of Journals. The manuscript for this paper was submitted for review and possible publication on March 19, 1986. This paper is part of the ***Journal of Waterway, Port, Coastal, and Ocean Engineering***, Vol. 113, No. 2, March, 1987. ©ASCE, ISSN 0733-950X/87/0002-0105/$01.00. Paper No. 21315.

of the previously constructed offshore breakwater systems (4,9,18, 25,26,27,29).

This paper presents small scale model tests for single offshore breakwaters with various breakwater lengths and offshore distances and for multiple offshore breakwaters with various gap spacings to examine the effects of their geometric parameters on the morphological change in their vicinity. The models in these tests were not scaled to match any particular prototype condition. There is still considerable debate concerning the scaling relationship of sediment models, and it was intended that model tests here were done in a consistent manner such that the relative merits of different geometric parameters of the breakwaters could be evaluated under the same conditions. The model results were compared with physical model studies reported by some other investigators, and the physical model tests were compared with the offshore breakwaters in the field.

Small Scale Model Tests

The small scale model tests were performed in a circular wave basin of 8.46 m diameter and 0.61 m height with a spiral wavemaker at its center. A spiral wavemaker in a circular basin simulates regular waves incident at a fixed angle on a long, straight shoreline. The readers who are not familiar with a spiral wavemaker are referred to Dalrymple and Dean (5), Mei (16), Dean and Dalrymple (8), Suh (24), and Trowbridge, et al. (28). Fig. 1 shows an experimental setup in the spiral wave basin. The spiral wavemaker used for the experiments is a 90-cm tall, 57.4-cm diameter steel drum mounted on a 3.81-cm diameter rotating shaft which is pully-driven by a 3-hp electric motor controlled by a DODGE SCR II Model 2300A controller. The offset of the rotating shaft from the axis of the drum is 3.81 cm. A sand beach with about a 1:5 overall slope was constructed along the basin wall. (The rapid radial decay of wave amplitude and incident angle prevents the use of a mild slope beach. This is the major disadvantage of a spiral wave basin.) The toe of the beach was located 1.7 m from the center of the basin and the water depth on the flat bottom was 0.4 m. The mean size and the standard deviation of the sand used for the experiments are 1.27 and 0.625, respectively, in phi units (relatively well-sorted medium sand), and its fall velocity in 20° C water is 5.5 cm/s with the assumption of $\rho_s = 2.65$, where ρ_s is the specific gravity of sand.

All the tests were performed for the wave period $T = 1.2$ sec. For a spiral wavemaker, this implies that the wave angle is fixed around the perimeter beach at a given distance from the wavemaker; here, the breaking wave angle is 2°. The values of the corresponding physical parameters on an equilibrium beach are as follows: H_0 (deepwater wave height) = 3.51 cm; L_0 (deepwater wavelength) = 2.25 m; H_b (breaking wave height) = 3.20 cm; h_b (water depth at breakerline) = 4.0 cm; r_b (distance from center of basin to breakerline) = 3.35 m; D (Dean number) = 0.532. The term Dean number is introduced here to refer to the dimensionless fall velocity, H_0/V_fT, where V_f = fall velocity of sand. The Dean number has been shown, by Dean (7) and Dalrymple and Thompson (6), to be extremely important in coastal processes. It indicates a typical normal beach profile (7) and this was confirmed through the ex-

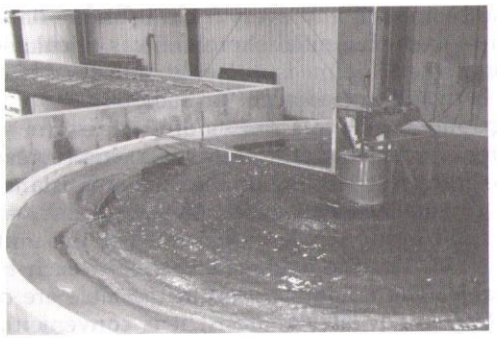

FIG. 1.—Experimental Setup in Spiral Wave Basin

periments. No offshore bar was observed and a step of about 2 cm height was formed along the breakerline. The breakerline and the uprush limit were located about 20 cm offshore and 15 cm onshore, respectively, from the still water line.

The wavemaker was run about 5 hr to obtain an equilibrium beach in the absence of any structure. A model offshore breakwater made of flexible hardboard was then placed in an equilibrium beach. Gravel was put on the seaward side of the breakwater to reduce reflected waves and to weaken the scour around the breakwater tips. The wavemaker was run again, and beach profile measurements were made at appropriate time intervals. The measurements were made at 0, 1, 2, 4, 6, and 8 hr for the tests 1–9 and 13–15 and at 0, 2, 4, 8, 12, and 16 hr for the tests 10–12, after the construction of the breakwater (Table 1). The total run time of the wavemaker was long enough to obtain a new equilibrium beach in the presence of the breakwater for most tests. The beach profiles were measured by means of a point gage installed on a radial carriage which rotated above the model area. The profile measurements were taken every

TABLE 1.—Test Description and Results of Present Study

Group (1)	Test number (2)	X_B (m) (3)	X_b (m) (4)	L_B (m) (5)	h_B (m) (6)	G_B (m) (7)	X_s (m) (8)	X_c (m) (9)	V_s ($m^3 \times 10^3$) (10)	V_d ($m^3 \times 10^3$) (11)	Remarks (12)
I	1	0.3	0.2	0.15	0.054		0.03	0.03	1.22	0.12	
	2	0.3	0.2	0.45	0.056		0.26	0.05	3.78	2.87	
	3	0.3	0.2	0.60	0.058		0.26	0.05	5.22	4.18	
	4	0.3	0.2	0.75	0.056		0.23	0.11	6.30	4.03	
	5	0.3	0.2	0.90	0.054		0.30	0.08	7.29	6.56	Tombolo
II	6	0.4	0.2	0.60	0.064		0.09	0.04	7.68	2.15	
	7	0.4	0.2	0.80	0.065		0.29	0.06	10.40	5.39	
	8	0.4	0.2	1.00	0.072		0.20	0.11	14.40	8.78	Double
	9	0.4	0.2	2.00	0.072		0.18	0.07	28.80	8.06	salients
III	10	0.5	0.2	1.00	0.095		0.15	0.09	23.75	6.18	
	11	0.5	0.2	1.25	0.087		0.22	0.09	27.19	7.34	
	12	0.5	0.2	1.50	0.100		0.21	0.15	37.50	9.00	
	13	0.4	0.2	1.00	0.071	0.5	0.16	0.11	14.20	4.83	Averaged
	14	0.4	0.2	1.00	0.074	1.0	0.27	0.11	14.80	6.96	values are
	15	0.4	0.2	1.00	0.069	2.0	0.16	0.08	13.80	3.45	used

20 cm along the basin wall and every 5 cm in the radial direction. The shoreline advance from the initial shoreline was calculated at each profile directly from the profile measurements, and the volumetric change was calculated between two adjacent profiles.

The test description and some results of the tests are summarized in Table 1. For later convenience, the tests for a single breakwater are divided into three groups depending on the offshore distance of the breakwater from the original still water line, X_B (group I: X_B = 0.3 m; group II: X_B = 0.4 m; and group III: X_B = 0.5 m). For the multiple offshore breakwater tests (13–15), the averaged values of each breakwater are shown in the table. The notations used in the table are defined in Appendix II and Fig. 2. For later analysis, it is convenient to define the following dimensionless variables developed in terms of X_B and V_s; $X_b^* = X_b/X_B$ = the dimensionless surf zone width; $X_s^* = X_s/X_B$ = the dimensionless salient amplitude, where X_s is measured from the original shoreline to the apex of the salient or tombolo; $L_B^* = L_B/X_B$ = dimensionless breakwater length; $G_B^* = G_B/X_B$ = the dimensionless gap width; $V_d^* = V_d/V_s$ = the dimensionless deposited volume, where $V_s = X_B L_B h_B/2$ = the total sheltered volume behind the breakwater, and h_B = the water depth at the breakwater.

Single Offshore Breakwater Tests.—The wave and current pattern and the morphological change near the breakwaters were observed visually, photographically, and by the profile measurements. The nearshore circulation pattern in the vicinity of the breakwater consists of longshore currents directed to the central part from both ends behind the breakwater which meet and generate an offshore current towards the breakwater. This offshore current separates and generates rip currents offshore around the breakwater tips, see Fig. 2. In most cases the currents

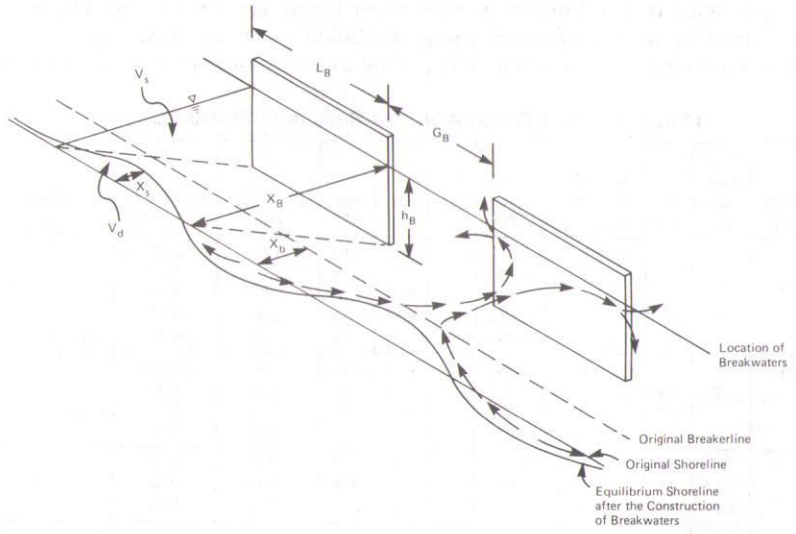

FIG. 2.—Schematic Diagram Illustrating Geometric Parameters and Current Patterns near Offshore Breakwater System

directly behind the breakwater were not large enough to initiate sand motion, so that initially a double-peak salient was formed. It was changed progressively into a single-peak salient by the offshore current. A typical result showing the temporal change of the shoreline near a single breakwater is shown in Fig. 3. The formation of a double-peak salient in the initial stage and its evolution into a single-peak salient can be seen in the figure. The results of the other tests are in Suh (24). In test 1 (L_B^* = 0.5), a very small salient was formed immediately after the construction

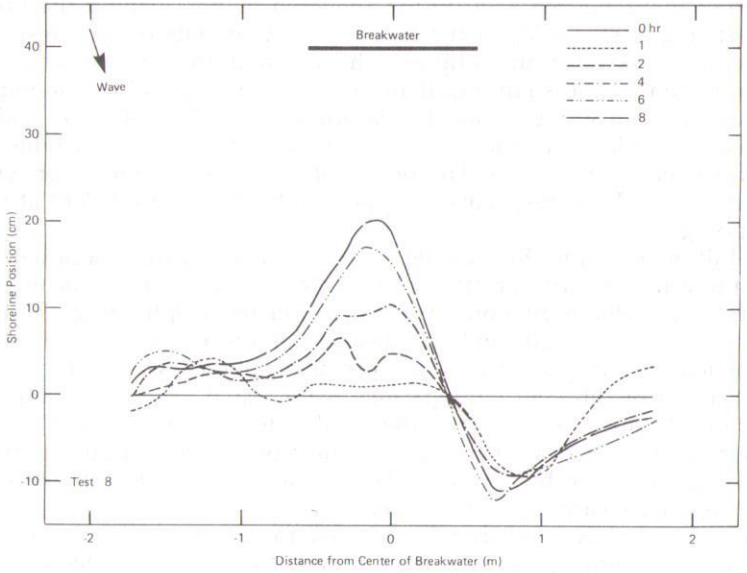

FIG. 3.—Shoreline Change (Test 8)

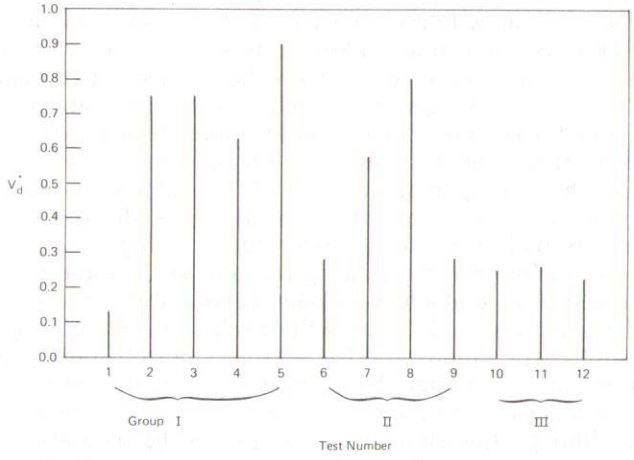

FIG. 4.—V_d^* at Final Equilibrium State of Each Test

of the breakwater, but it never grew. A tombolo was formed in test 5 ($L_B^* = 3.0$). But in the tests in group II or III, in which the location of the breakwater was relatively far offshore, a tombolo was never formed, although L_B^* was greater than or equal to 3.0. In test 9, in which the length of the breakwater was very long compared with its offshore distance ($L_B^* = 5.0$), a permanent double-peak salient with a lagoon in the middle was formed.

One possible measure of the sand-trapping capacity of an offshore breakwater is the dimensionless value V_d^*, which is the ratio of the volume of the deposited sand to the sheltered volume behind the breakwater. Fig. 4 shows V_d^* at the final equilibrium state of each test. The offshore breakwaters in group III, which were in the deepest water, appear to be much less efficient than those in groups I and II. Among the breakwaters in groups I and II, six breakwaters (2, 3, 4, 5, 7, and 8), considered relatively efficient, show similar value of V_d^*, for which L_B^* lies between 2.0 and 3.0. The breakwaters in tests 5 and 8 for which L_B^* are 3.0 and 2.5, respectively, appear to be the most efficient at sand trapping.

Multiple Offshore Breakwater Tests.—If a large extent of beach is to be protected, a series of offshore breakwaters can be constructed. The effects of multiple offshore breakwaters on the neighboring shoreline depend on the length and the distance of the breakwaters from the shoreline and the gap spacing between adjacent breakwaters. Here, only the effects of different gap spacings were tested. The length and the distance from the shoreline of the breakwaters were fixed as those for test 8, which was demonstrated to be the most efficient at sand trapping for single offshore breakwaters. Three tests (13–15) with different gap spacings were carried out (Table 1).

Fig. 5(*a–c*) shows the shoreline change in each test. The erosion and accretion pattern in test 15 is quite different from those in tests 13 and 14. The wave pattern and the wave height behind the gap are related to the wavelength as well as the gap spacing. The wavelength at the location of the breakwater was 0.95 m. In test 15, in which the gap spacing was approximately twice the wavelength, the shoreline behind each breakwater responded independently, as if there were no interaction among the breakwaters (compare with the results of the single breakwater in Fig. 3), and a log-spiral shoreline was formed at the downdrift beach of each breakwater. The maximum shoreline advance or recession was somewhat smaller than that of the single breakwater. For tests 13 and 14 in which the gap spacing was 1/2 or almost the same as the wavelength, the erosion pattern behind the gaps showed a circular or elliptic feature with its center at the center of each gap.

In test 14 in which the gap spacing was almost the same as one wavelength, a complete tombolo was built behind the furthest downdrift breakwater after 4 hr and the growth of salient decreased updrift. This is opposite to expectations and the reason is not obvious. This continuous growth of salient might be because the shoreline tends to make an equilibrium state in accordance with the circular wave pattern behind the gap. Although this shoreline pattern could be seen also in test 13, the insufficient sand supply from the eroded area [*B*, *D*, *F* in Fig. 5(*a*)] prevented the salients from growing after about 4 hr.

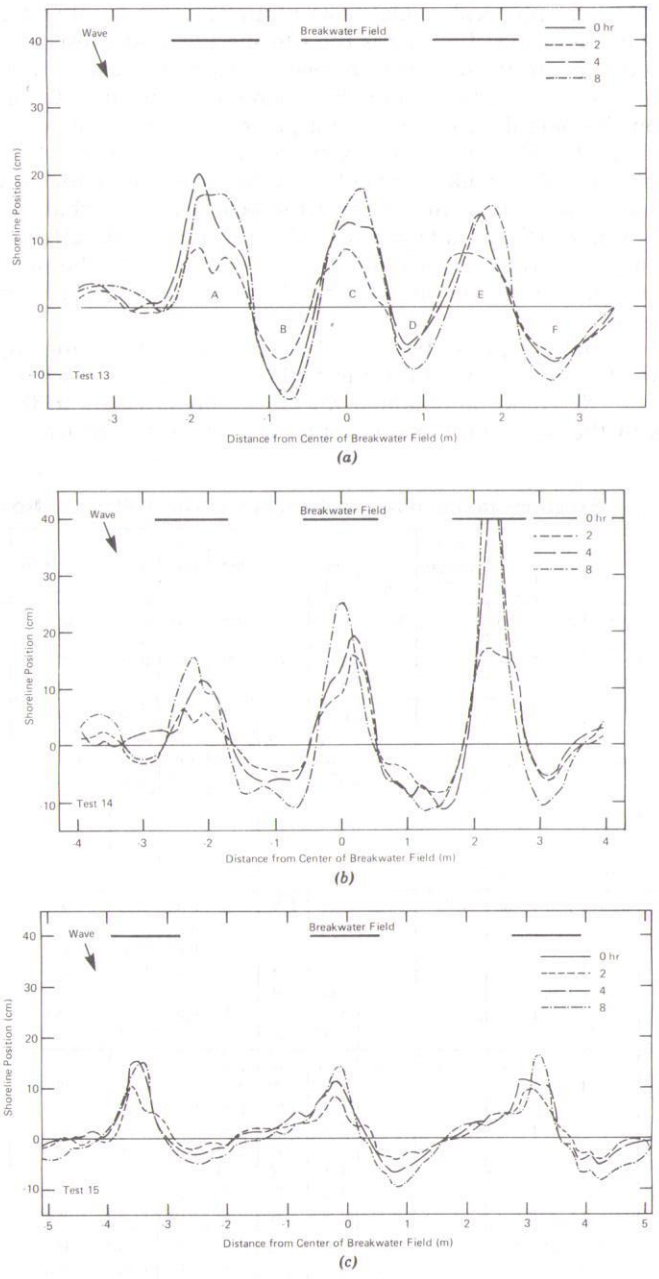

FIG. 5.—Shoreline Change: (*a*) Test 13; (*b*) Test 14; (*c*) Test 15

Comparison with Other Physical Model Tests and Field Projects

Two kinds of physical model tests of an offshore breakwater system have been conducted. The first is the site-specific model tests (1,2,3,9,22), and the others are those that have been designed to examine and compare the effects of various geometric parameters of an offshore breakwater on the neighboring beach in a given wave and bathymetric condition (21,23,24). The present study concentrates upon the latter unscaled model studies. The available data from other physical model studies are summarized in Table 2. In the table the beach slope is that of the premolded beach. All the data in the table are for a single offshore breakwater subject to normal incident waves. Additionally, the summary of the characteristics of the offshore breakwaters in the field is presented in Table 3.

The parameter representing the degree of sand-capturing capacity of a breakwater differs from author to author. As the dimensionless salient amplitude, X_s^* could be obtained for all the breakwaters in the field as well as in the laboratory experiments, it was chosen in this study. To

TABLE 2.—Experimental Condition and Results of Other Physical Model Tests

Author (1)	T (s) (2)	H_0 (cm) (3)	L_0 (m) (4)	Dean number (5)	m (6)	X_B (m) (7)	X_b (m) (8)	L_B (m) (9)	h_B (m) (10)	X_s (m) (11)	V_s ($m^3 \times 10^3$) (12)	V_d ($m^3 \times 10^3$) (13)
Shinohara and Tsubaki (1966)	0.922	2.55	1.33	0.61	0.067	0.75	1.60	1.50	0.05	0.27	28.1	17.7
						1.50	1.60	1.50	0.10	0.31	112.5	17.0
						2.65	1.60	1.50	0.18	0.35	357.8	18.1
						3.75	1.60	1.50	0.25	0.33	703.1	15.3
		6.13	1.33	1.48	0.067	0.75	1.60	1.50	0.05	0.50	28.1	28.8
						1.50	1.60	1.50	0.10	0.58	112.5	45.0
						2.65	1.60	1.50	0.18	0.41	357.8	43.5
						3.75	1.60	1.50	0.25	0.20	703.1	15.3
Horikawa and Koizumi (1974)	1.15	5.51	2.06			2.00		4.00		1.07		
Rosen and Vajda (1982)	0.80	1.50	1.00	0.65	0.025	3.00	1.36	0.50	0.08	0.16	60.0	
						3.00	1.36	1.00	0.08	0.26	120.0	
						3.00	1.36	2.00	0.08	0.38	240.0	
						2.00	1.36	0.50	0.05	0.21	25.0	
						1.00	1.36	0.50	0.03	0.24	7.5	
						1.00	1.36	1.00	0.03	0.56	15.0	
						1.00	1.36	2.00	0.03	0.82	30.0	
	1.00	3.90	1.56	1.34	0.033	2.50	1.70	1.00	0.08	0.35	100.0	
						2.00	1.70	0.50	0.07	0.23	35.0	
						2.00	1.70	1.00	0.07	0.42	70.0	
						2.00	1.70	2.00	0.07	0.66	140.0	
						1.00	1.70	0.50	0.03	0.26	7.5	
						1.00	1.70	1.00	0.03	0.55	15.0	
						1.00	1.70	2.00	0.03	1.00	30.0	
						1.00	1.70	0.50	0.03	0.25	7.5	
	1.15	8.00	2.06	2.40	0.040	2.00	1.00	0.50	0.08	0.05	40.0	
						2.00	1.00	1.00	0.08	0.24	80.0	
						2.00	1.00	2.00	0.08	0.23	160.0	
Mimura, et al. (1983)	0.90	5.70	1.26	2.75	0.050	1.80	1.80	1.50	0.09	0.65	121.5	69.6

confirm this, V_d^* versus X_s^* is shown in Fig. 6. For the multiple offshore breakwaters, the averaged values were used. If we approximate the area of a salient as $L_B X_s/2$, and the water depth at the apex of the salient as mX_s in which m = the beach slope, V_d can be expressed by

$$V_d = \frac{\alpha m L_B X_s^2}{4} \quad \ldots\ldots (1)$$

in which α (≥ 1) = a deposition factor which takes into account the deposition of sand both above the water level and underwater in the vicinity of the salient. By using the definition of V_s, V_d^*, and X_s^*, we have

$$V_d^* = \frac{\alpha X_s^{*2}}{2} \quad \ldots\ldots (2)$$

This relationship is shown in Fig. 6 for α = 1, 2, 4, and 8. Most of the laboratory data, X_s^* of which is approximately greater than 0.5, lie near the line of α = 2. The offshore breakwater system in Kaike, Japan, also shows α around 2. All the field data quoted from Nir (18) show α less than 2. This is because he did not take into account the sand deposition above the water level and underwater. He reported that the underwater volume is almost the same as the visible volume, which is presented in Table 3. Thus, Nir's data will be located near the line of α = 2, if the underwater volume is included.

Several previous investigators (21,23) attempted to find the dependence of the sand deposition behind an offshore breakwater upon L_B^*. On the other hand, Rosen and Vajda (21) showed its dependence on X_b^* based on their and some others' experimental results. This is the case also in the field, see Toyoshima (26). Fig. 7 shows the relation between L_B^* and X_s^* in the laboratory experiments and the field. To see the dependence on X_b^*, the experimental data are divided into 3 groups depending on the extent of X_b^*. The best fitting lines intersecting the origin are calculated for each group as follows:

$$X_s^* = 0.156 L_B^*; \quad X_b^* < 0.5; \quad R = 0.98; \quad X_s^* = 0.317 L_B^*; \quad 0.5 \leq X_b^* < 1.0;$$

$$R = 0.85; \quad X_s^* = 0.377 L_B^*; \quad X_b^* \geq 1.0; \quad R = 0.75 \quad \ldots\ldots (3)$$

in which R = the correlation coefficient. For each group the increase of X_s^* with that of L_B^* is clearly shown although the data tend to scatter for larger values of X_b^*. The sand-capturing capacity of the breakwaters with values of X_b^* less than 0.5 is much less than that of those with larger values of X_b^*. For the breakwaters with X_b^* larger than 0.5, the effects of X_b^* are not so clear. In the field the shoreline behind a breakwater advances much further offshore than that in the laboratory experiments for the same value of L_B^* so that a tombolo is formed for the value of L_B^* greater than about one. The only exception is the Santa Monica breakwater in California for which L_B^* = 1.0, but X_s^* is only 0.39. This is in part because the breakwater is located much farther offshore (X_B = 610 m) compared with other breakwaters. The dependence of X_s^* on X_b^* could not be shown for the breakwaters in the field, since the wave condition and the corresponding breaker point are not constant in the field. But

TABLE 3.—Summary of Characteristics of Offshore Breakwaters in Field

Breakwater type (1)	Author (2)	Location (3)	Number of segments (4)	Name of breakwater[a] (5)	X_B (m) (6)	L_B (m) (7)	h_B (m) (8)	G_B (m) (9)	m (10)	X_s (m) (11)	V_s (m^3) (12)	V_d (m^3) (13)	Remarks (14)
Single	Nir (1982), and Rosen and Vajda (1982)	Haifa, Israel		Hof Hacarmel	200	280	3.0		0.015	200	84,000	55,000	
		Nahariyya, Israel		Nahariyya	70	180	3.2		0.046	70	20,160	20,000	Groins in its neighborhood
		Tel Aviv, Israel		Tel Baruch	100	200	3.0		0.030	100	30,000	15,000	
	Dally and Pope (1985)	Venice, CA		Venice	370	180	1.8		0.005	170	59,940		Before 1940
					210	180				210			After beach fill during 1940's
		Santa Monica, CA		Santa Monica	610	610	8.4		0.014	240			
		Haleiwa, HI		Haleiwa	50	50	2.1		0.042	45			Beach fill placed
Segmented	Walker, et al. (1980)	Lorain, OH	3	West	76	76	2.4	31	0.032		6,931	−2,140	Beach fill placed
				Center	72	76	2.4	31	0.033		6,566	3,058	
				East	72	76	2.4	31	0.033		6,566	3,428	
				Average	73	76	2.4	31	0.033		6,688	1,450	
	Fried (1976), Nir (1982), and Rosen and Vajda (1982)	Netanya, Israel	2	South	216	240	3.5	112	0.016	216	90,720	38,000	
				North	200	207	3.5	112	0.018	200	72,450	34,000	
				Average	208	224	3.5	112	0.017	208	81,585	36,000	
		Tel Aviv, Israel	2	Sheraton	200	310	4.0	150	0.020	200	124,000	45,000	T-shape breakwater
				Hilton	200	240	4.0	150	0.020	200	96,000	20,000	
				Average	200	275	4.0	150	0.020	200	110,000	32,500	
	Toyoshima (1982)	Kaike, Japan	11	Kaike 1	110	150	5.0	50	0.045	110	41,250	35,800	
				Kaike 2	110	150	5.0	50	0.045	110	41,250	48,800	
				Kaike 3	145	150	4.5	50	0.031	113	48,940	18,300	
				Kaike 4	100	150	5.0	50	0.050	100	37,500	45,000	
				Kaike 5	140	150	3.0	50	0.021	140	31,500	18,900	
				Kaike 6	100	150	5.0	50	0.050	100	37,500	28,900	
				Kaike 7	155	150	3.0	50	0.019	119	34,880	24,800	
				Kaike 8	115	150	2.5	50	0.022	115	21,560	15,300	
				Kaike 9	100	150	3.0	50	0.030	100	22,500	13,400	
				Kaike 10	75	150	3.0	50	0.040	75	16,880	28,300	
				Kaike 11	75	150	2.5	50	0.033	36	14,060	7,400	
				Average	111	150	3.8	50	0.034	102	31,640	25,900	
	Dally and Pope (1985)	Presque Isle, PA	3	West	45	40	1.0	90	0.022	31	900		Beach fill placed
				Center	60	40	1.0	75	0.017	12	1,200		
				East	60	40	1.0	60	0.017	6	1,200		
				Average	55	40	1.0	75	0.018	16	1,100		
		Colonial Beach, VA	4	Central 1	65	60	1.2	45	0.018	61	2,340		Beach fill placed
				Central 2	65	60	1.2	45	0.018	62	2,340		
				Central 3	65	60	1.2	45	0.018	59	2,340		
				Central 4	65	60	1.2	45	0.018	61	2,340		
				Average	65	60	1.2	45	0.018	61	2,340		

TABLE 3.—

(1)	(2)	(3)	(4)	(5)	(6)
			3	Castlewood 1	24
				Castlewood 2	24
				Castlewood 3	24
				Average	24

[a]Some of the breakwater names were given by the present authors.

the data for the Santa Monica breakwater confirms, at least qualitatively, the importance of X_B^* even in the field.

Multiple offshore breakwaters have been used in many places for the protection of extensive coastal areas, but the physical model studies of them have been scarcely made. The previously mentioned results of the present model study show the importance of the gap spacing G_B on the shoreline response behind multiple breakwaters. Since the breakwater length is also an important factor, we introduce a dimensionless quantity, G_B^*/L_B^{*2}, which includes all the effects of G_B, L_B, and X_B. Fig. 8 shows the relation between G_B^*/L_B^{*2} and the dimensionless salient amplitude X_s^*, in the present model tests and several field projects. In the figure, the curve approximately fitting the field data is given by

$$X_s^* = 14.8\left(\frac{G_B^*}{L_B^{*2}}\right)\exp\left[-2.83\left(\frac{G_B^*}{L_B^{*2}}\right)^{1/2}\right] \quad \ldots\ldots\ldots\ldots\ldots\ldots\ldots\ldots\ldots\ldots\ldots\ldots (4)$$

which has its peak at $G_B^*/L_B^{*2} = 0.5$. The averaged value behind each breakwater were used for the plot. For the data quoted from Dally and

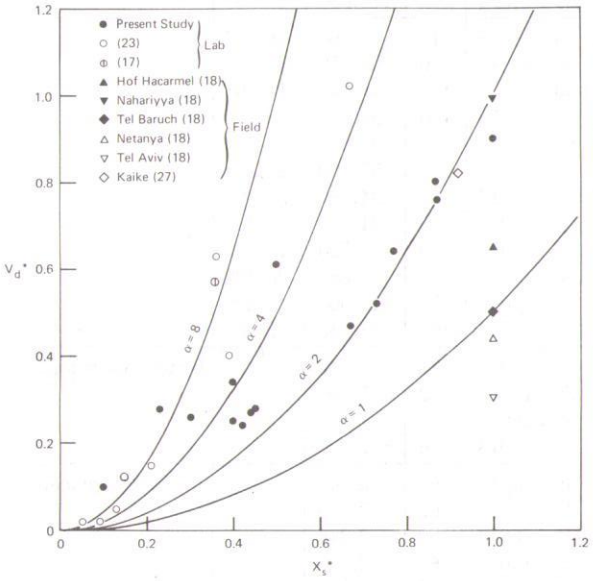

FIG. 6.—Relation between X_s^* and V_d^*

Continued

(7)	(8)	(9)	(10)	(11)	(12)	(13)	(14)
90	0.9	40	0.038	24	972		Beach fill placed
60	0.9	33	0.038	14	648		
60	0.9	26	0.038	8	648		
70	0.9	33	0.038	15	756		

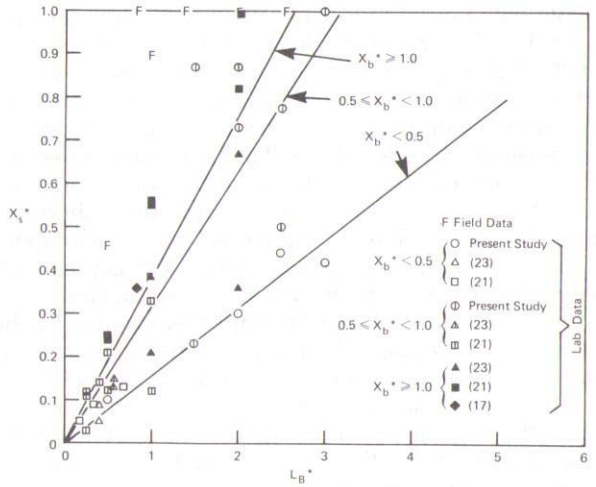

FIG. 7.—Relation between L_B^* and X_s^* for Single Offshore Breakwaters

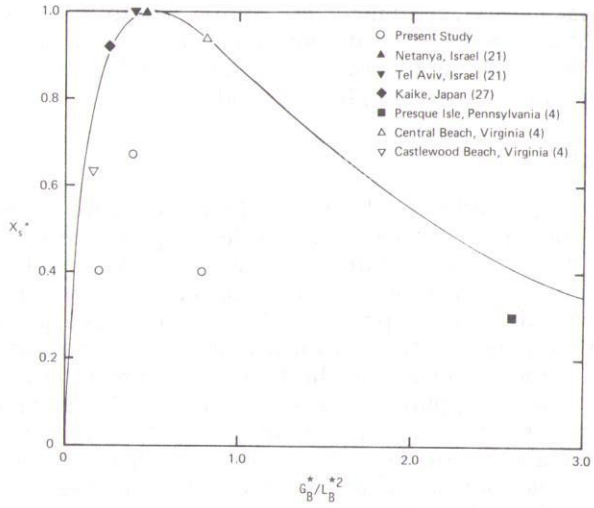

FIG. 8.—Relation between G_B^*/L_B^{*2} and X_s^*

Pope (4), X_s^* was calculated from the aerial photographs presented in their report. In the places where beach fill was used, X_s was measured from the shoreline just after the beach fill. Generally, X_s^* increases as G_B^*/L_B^{*2} decreases with the greatest X_s^* for G_B^*/L_B^{*2} around 0.5, and then decreases rapidly towards zero for the smaller values of G_B^*/L_B^{*2}. The same trend is shown for both the laboratory tests and the field, although the value of X_s^* in the field is greater than that in the laboratory tests for the same value of G_B^*/L_B^{*2}. Tombolos are formed for G_B^*/L_B^{*2} around 0.5 in the field. The physical interpretation of the dimensionless quantity G_B^*/L_B^{*2} is instructive. In dimensional form, it can be expressed as $G_B X_B/L_B^2$. For a finite value of G_B, this quantity approaches zero for small X_B or large L_B, and in this case tombolos are formed ($X_s^* = 1$). If X_B is large or L_B is small, $G_B X_B/L_B^2$ becomes bigger, and the salient amplitude reduces. Similar arguments can be made for G_B with finite values of X_B and L_B. For larger value of G_B, its effects on the shoreline change are negligible because each breakwater will behave independently as if there were no interaction among the breakwaters. However, for relatively small value of G_B, the wave field and the corresponding shoreline configuration behind the gap are largely influenced by the gap spacing. Especially, if G_B is so small that the erosion behind the gap is negligible, the resulting growth of the salients is also very insignificant.

As shown in Figs. 7 and 8, the offshore breakwaters in the field are more efficient at sand trapping than those in the laboratory experiments for the same geometric similitudes, so that X_s^* in the field is larger than that in the laboratory experiments for the same value of L_B^* or G_B^*/L_B^{*2}. In addition to these geometric parameters, the growth of salients and the formation of tombolos will depend on the beach slope and the Dean number. Different beach slopes will alter the wave field behind the breakwaters through wave refraction, which in turn will change the shape of the salients. The Dean number represents the dynamic similitude between waves and sediments. Both the beach slopes and the Dean numbers in the laboratory experiments are comparable to those in the field (Tables 2 and 3). Possibly, this difference between the laboratory experiments and the field might be caused by the variability of real wave climate and the use of unscaled physical models.

Conclusions

The use of single and multiple offshore breakwaters for the beach protection was examined in terms of various design parameters. Laboratory model tests were compared with the breakwaters in the field to show, for a single offshore breakwater, that L_B^* appears to be an important parameter for effective sand trapping, so that X_s^* increases as L_B^* does. Another important parameter is the dimensionless surf zone width X_b^*, so that the closer the breakwater to the shoreline the more efficient is the breakwater at sand trapping for the same value of L_B^*. For multiple offshore breakwaters, the dimensionless quantity G_B^*/L_B^{*2} appears to be an important parameter for its effectiveness, so that X_s^* increases as G_B^*/L_B^{*2} decreases until G_B^*/L_B^{*2} reaches about 0.5 and over the point X_s^* decreases rapidly with G_B^*/L_B^{*2}.

The offshore breakwaters in the field are much more efficient in terms

of X_s^* than those in the laboratory experiments for the same value of L_B^* or G_B^*/L_B^{*2}. In the field a tombolo is usually formed behind a single breakwater for $L_B^* \geq 1$ if the breakwater is not located too far offshore. For a multiple offshore breakwater, tombolos are formed when G_B^*/L_B^{*2} is about 0.5.

The unscaled model tests themselves give reasonably consistent relationships between the geometric parameters of the offshore breakwaters and the resulting morphological changes. However, their comparison with the breakwaters in the field shows considerable difference, which might be caused from the variability of real wave climate and scale effects in laboratory tests. Several empirical relationships (Eqs. 2, 3, and 4) were drawn from a limited data set, which could give good guidelines to the future construction of offshore breakwater systems. Monitoring of existing offshore breakwater systems also can give additional guidance in general, but a properly scaled physical model can provide important insights into the site-specific requirements of the design.

Acknowledgments

This work is partly a result of research sponsored by NOAA Office of Sea Grant, Department of Commerce, under Grant No. NA83AA-D-0017 (Project No. 3-7-21-3120-31). The U.S. Government is authorized to produce and distribute reprints for governmental purposes, notwithstanding any copyright notation that may appear herein.

Appendix I.—References

1. Bottin, R. R., "Lakeview Park Beach Erosion Study, Ohio," *Letter Report*, U.S. Army Engineer Waterways Experiment Station, Coastal Engineering Research Center, Vicksburg, Miss., 1982.
2. Curren, C. R., and Chatham, C. E., "Imperial Beach, California, Design of Structures for Beach Erosion Control: Hydraulic Model Investigation," *Technical Report H-77-15*, U.S. Army Engineer Waterways Experiment Station, Coastal Engineering Research Center, Vicksburg, Miss., 1977.
3. Curren, C. R., and Chatham, C. E., "Oceanside Harbor and Beach, California, Design of Structures for Harbor Improvement and Beach Erosion Control: Hydraulic Model Investigation," *Technical Report HL-80-10*, U.S. Army Engineer Waterways Experiment Station, Coastal Engineering Research Center, Vicksburg, Miss., 1980.
4. Dally, W. R., and Pope, J., "Detached Breakwaters for Shore Protection," *Technical Report CERC-86-1*, U.S. Army Engineer Waterways Experiment Station, Coastal Engineering Research Center, Vicksburg, Miss., 1986.
5. Dalrymple, R. A., and Dean, R. G., "The Spiral Wavemaker for Littoral Drift Studies," *Proceedings of the 13th Coastal Engineering Conference*, ASCE, Vol. 1, 1972, pp. 689–705.
6. Dalrymple, R. A., and Thompson, W. W., "Study of Equilibrium Beach Profiles," *Proceedings of the 15th Coastal Engineering Conference*, ASCE, Vol. 2, 1976, pp. 1277–1296.
7. Dean, R. G., "Heuristic Models of Sand Transport in the Surf Zone," *First Australian Conference on the Engineering Dynamics of the Coastal Zone*, Institution of Engineers, Australia, 1973, pp. 208–215.
8. Dean, R. G., and Dalrymple, R. A., *Water Wave Mechanics for Engineers and Scientists*, Prentice-Hall, Inc., Englewood Cliffs, N.J., 1984.
9. Fried, I., "Protection by Means of Offshore Breakwaters," *Proceedings of the*

15th Coastal Engineering Conference, ASCE, Vol. 2, 1976, pp. 1493–1512.
10. Gourlay, M. R., "Non-uniform Alongshore Currents," *Proceedings of the 15th Coastal Engineering Conference*, ASCE, Vol. 1, 1976, pp. 701–720.
11. Gourlay, M. R., "Wave Set-up and Wave Generated Currents in the Lee of a Breakwater or Headland," *Proceedings of the 14th Coastal Engineering Conference*, ASCE, Vol. 3, 1974, pp. 1976–1995.
12. Horikawa, K., and Koizumi, C., "An Experimental Study on the Function of an Offshore Breakwater," *29th Annual Conference*, Japanese Society of Civil Engineers, 1974, pp. 85–87.
13. Kraus, N. C., "Application of a Shoreline Prediction Model," *Proceedings of Coastal Structures '83*, ASCE, Vol. 2, 1983, pp. 632–645.
14. Liu, P. L-F., and Mei, C. C., "Effects of a Breakwater on Nearshore Currents Due to Breaking Waves," *Technical Memorandum No. 57*, U.S. Army, Corps of Engineers, Coastal Engineering Research Center, Fort Belvoir, Va., 1975.
15. Matsuoka, M., and Ozawa, Y., "Application of a Numerical Model to Prediction of Shoreline Changes," *Proceedings of Coastal Structures '83*, ASCE, Vol. 2, 1983, pp. 646–659.
16. Mei, C. C., "Shoaling of Spiral Waves in a Circular Basin," *Journal of Geophysical Research*, Vol. 78, No. 6, Feb., 1973, pp. 977–980.
17. Mimura, N., Shimizu, T., and Horikawa, K., "Laboratory Study on the Influence of Detached Breakwater on Coastal Change," *Proceedings of Coastal Structures '83*, ASCE, Vol. 2, 1983, pp. 740–752.
18. Nir, Y., "Offshore Artificial Structures and Their Influence on the Israel and Sinai Mediterranean Beaches," *Proceedings of the 18th Coastal Engineering Conference*, ASCE, Vol. 3, 1982, pp. 1837–1856.
19. Penney, W. G., and Price, A. T., "The Diffraction Theory of Sea Waves and the Shelter Afforded by Breakwaters," *Philosophical Transactions of the Royal Society*, Series A, Vol. 244(882), 1952, pp. 236–253.
20. Perlin, M., "Predicting Beach Planforms in the Lee of a Breakwater," *Proceedings of Coastal Structures '79*, ASCE, Vol. 2, 1979, pp. 792–808.
21. Rosen, D. S., and Vajda, M., "Sedimentological Influences of Detached Breakwaters," *Proceedings of the 18th Coastal Engineering Conference*, ASCE, Vol. 3, 1982, pp. 1930–1949.
22. Seabergh, W. C., "Design for Prevention of Beach Erosion at Presque Isle, Erie, Pennsylvania," *Technical Report HL-83-15*, U.S. Army Engineer Waterways Experiment Station, Coastal Engineering Research Center, Vicksburg, Miss., 1983.
23. Shinohara, K., and Tsubaki, T., "Model Study on the Change of Shoreline of Sandy Beach by the Offshore Breakwater," *Proceedings of the 10th Coastal Engineering Conference*, ASCE, Vol. 1, 1966, pp. 550–563.
24. Suh, K., "Modeling of Beach Erosion Control Measures in a Spiral Wave Basin," thesis presented to the University of Delaware, at Newark, Del., in 1985, in partial fulfillment of the requirements for the degree of Master of Civil Engineering.
25. Toyoshima, O., "Changes of Sea Bed Due to Detached Breakwaters," *Proceedings of the 15th Coastal Engineering Conference*, ASCE, Vol. 2, 1976, pp. 1572–1589.
26. Toyoshima, O., "Design of a Detached Breakwater System," *Proceedings of the 14th Coastal Engineering Conference*, ASCE, Vol. 2, 1974, pp. 1419–1431.
27. Toyoshima, O., "Variation of Foreshore Due to Detached Breakwaters," *Proceedings of the 18th Coastal Engineering Conference*, ASCE, Vol. 3, 1982, pp. 1873–1892.
28. Trowbridge, J., Dalrymple, R. A., and Suh, K., "A Simplified Second Order Solution for a Spiral Wavemaker," *Journal of Geophysical Research*, Vol. 91, No. C10, Oct., 1986, pp. 11783–11789.
29. Walker, J. R., Clark, D., and Pope, J., "A Detached Breakwater System for Beach Protection," *Proceedings of the 17th Coastal Engineering Conference*, ASCE, Vol. 2, 1980, pp. 1968–1987.

APPENDIX II.—NOTATION

The following symbols are used in this paper:

D = Dean number;
G_B = gap width between adjacent breakwaters;
H_b = breaking wave height;
H_0 = deepwater wave height;
h_B = water depth at breakwater;
h_b = water depth at breakerline;
L_B = breakwater length;
L_0 = deepwater wavelength;
m = beach slope;
r_b = distance from center of circular basin to breakerline;
T = wave period;
V_d = volume of sand deposited behind breakwater;
V_f = fall velocity of sediment;
V_s = sheltered volume behind breakwater;
X_B = offshore distance of breakwater;
X_b = surf zone width;
X_e = maximum downdrift erosion;
X_s = salient amplitude;
α = deposition factor; and
ρ_s = specific gravity of sediment.

Superscript

$*$ = a dimensionless quantity.